

Figure S1. the two conformers of cyano-ester oligothiophenes considered in this work.

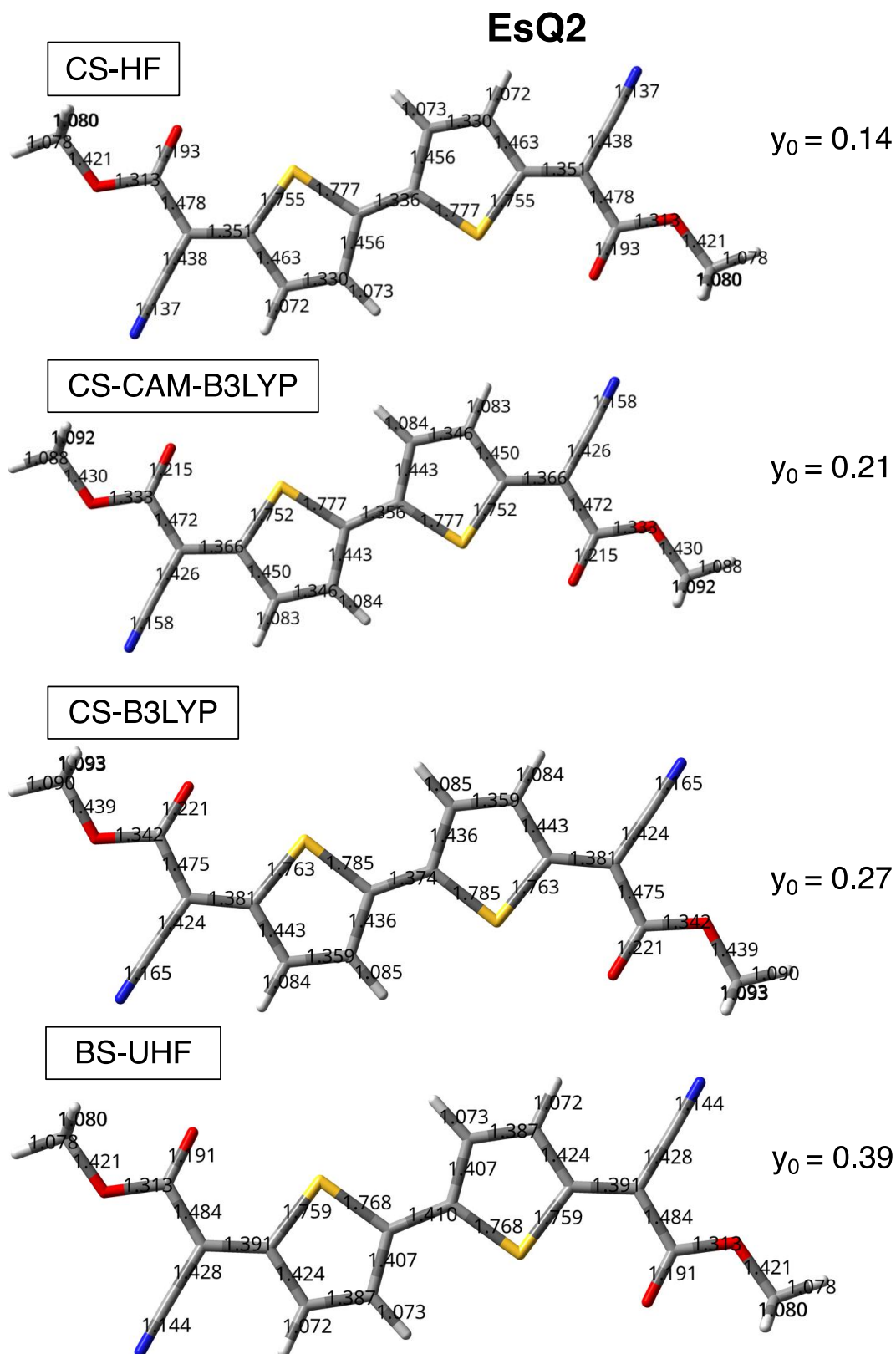


Figure S2. Library of ground state geometries generated for **EsQ2** and the corresponding y_0^{PUHF} value. The level of theory is indicated. The basis set is always 6-31G*.

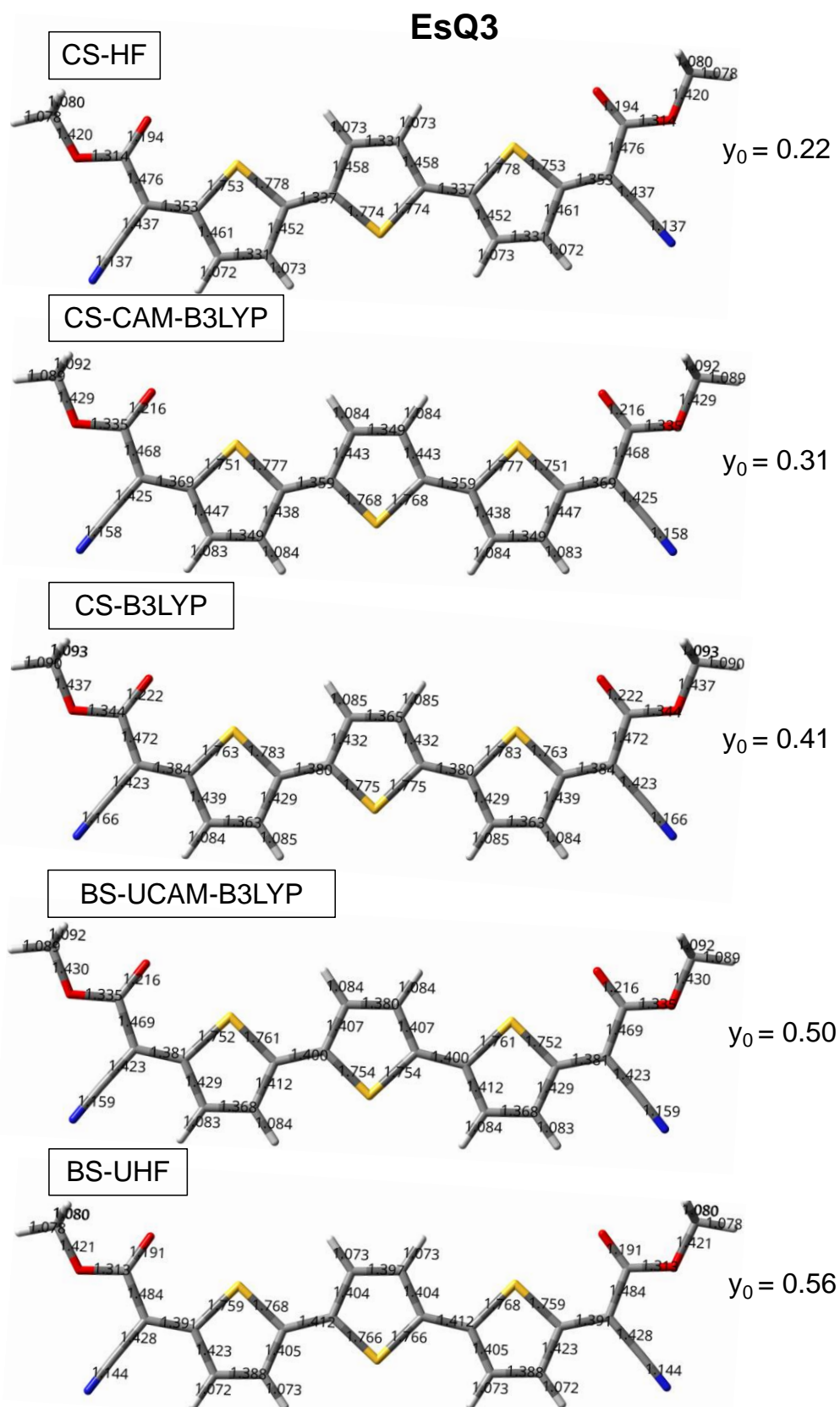


Figure S3. Library of ground state geometries generated for EsQ3 and the corresponding y_0^{PUHF} value. The level of theory is indicated. The basis set is always 6-31G*.

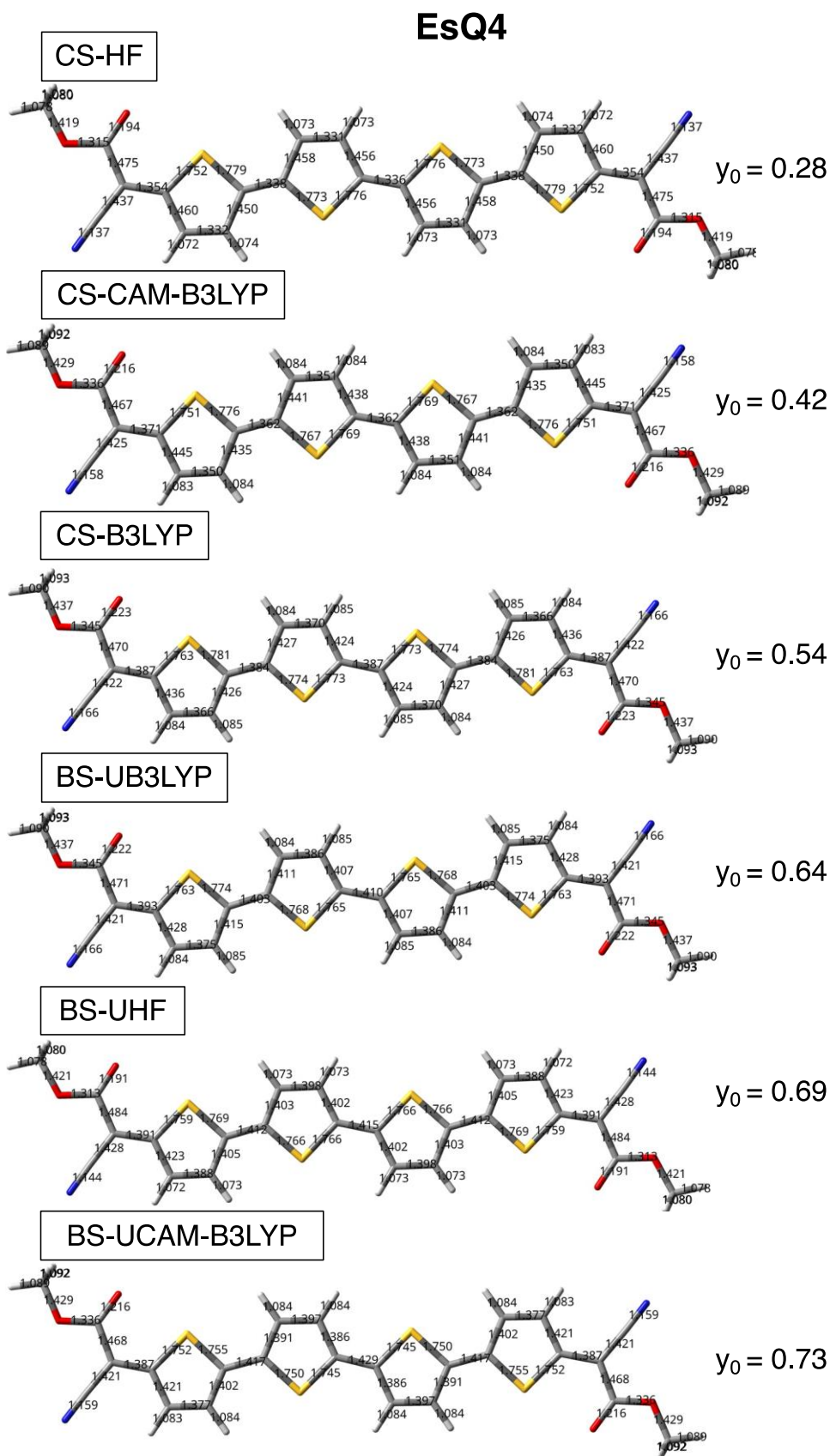


Figure S4. Library of ground state geometries generated for **EsQ4** and the corresponding y_0^{PUHF} value. The level of theory is indicated. The basis set is always 6-31G*.

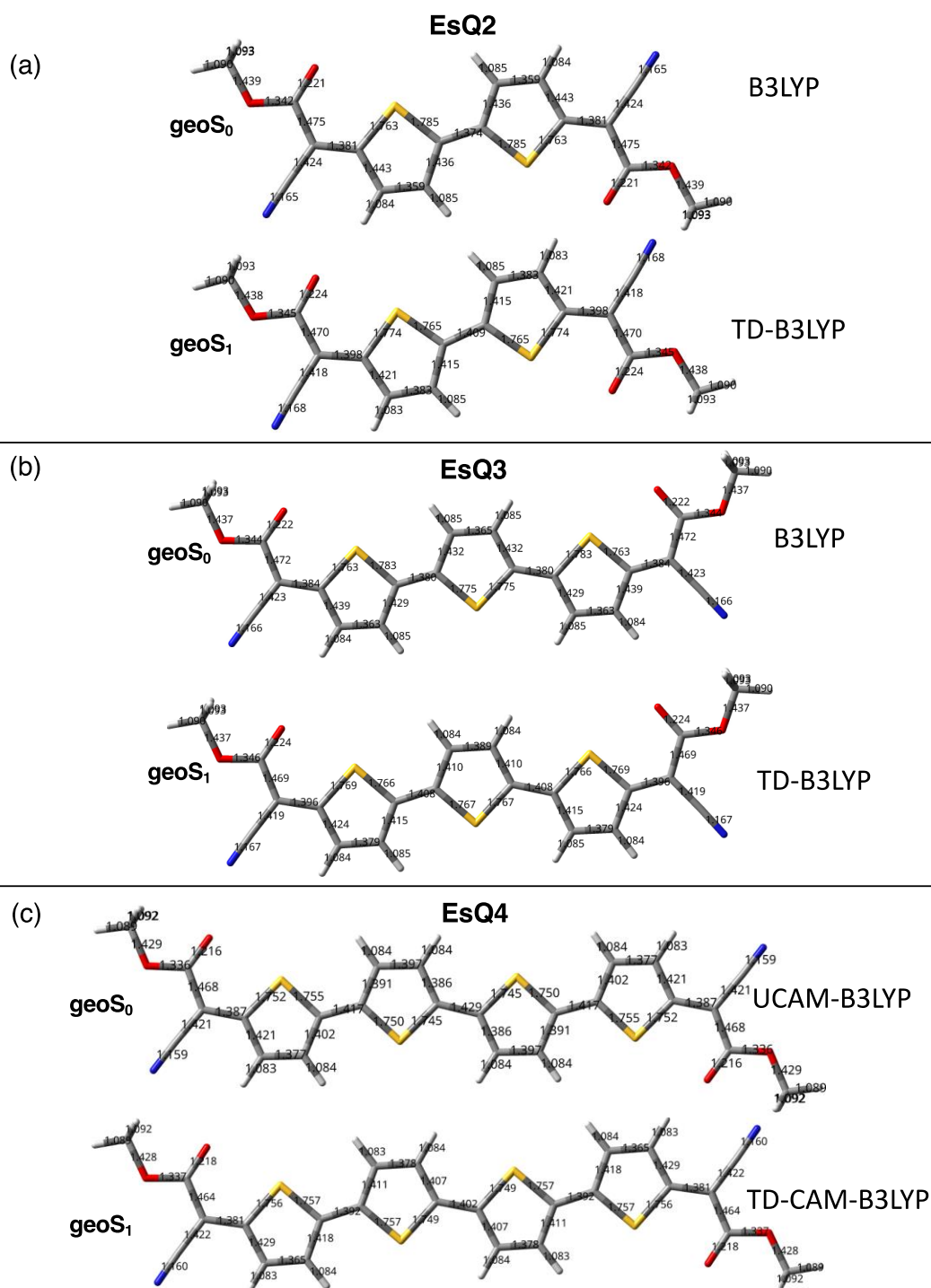


Figure S5. Comparison between ground state and excited state structure (optically active state dominated by the HOMO \rightarrow LUMO excitation) of **EsQ2**-**EsQ4** oligomers. The equilibrium structures were determined at CS-B3LYP / TD-B3LYP level for **EsQ2** and **EsQ3** and at BS-UCAM-B3LYP / TD-CAM-B3LYP level for **EsQ4**.

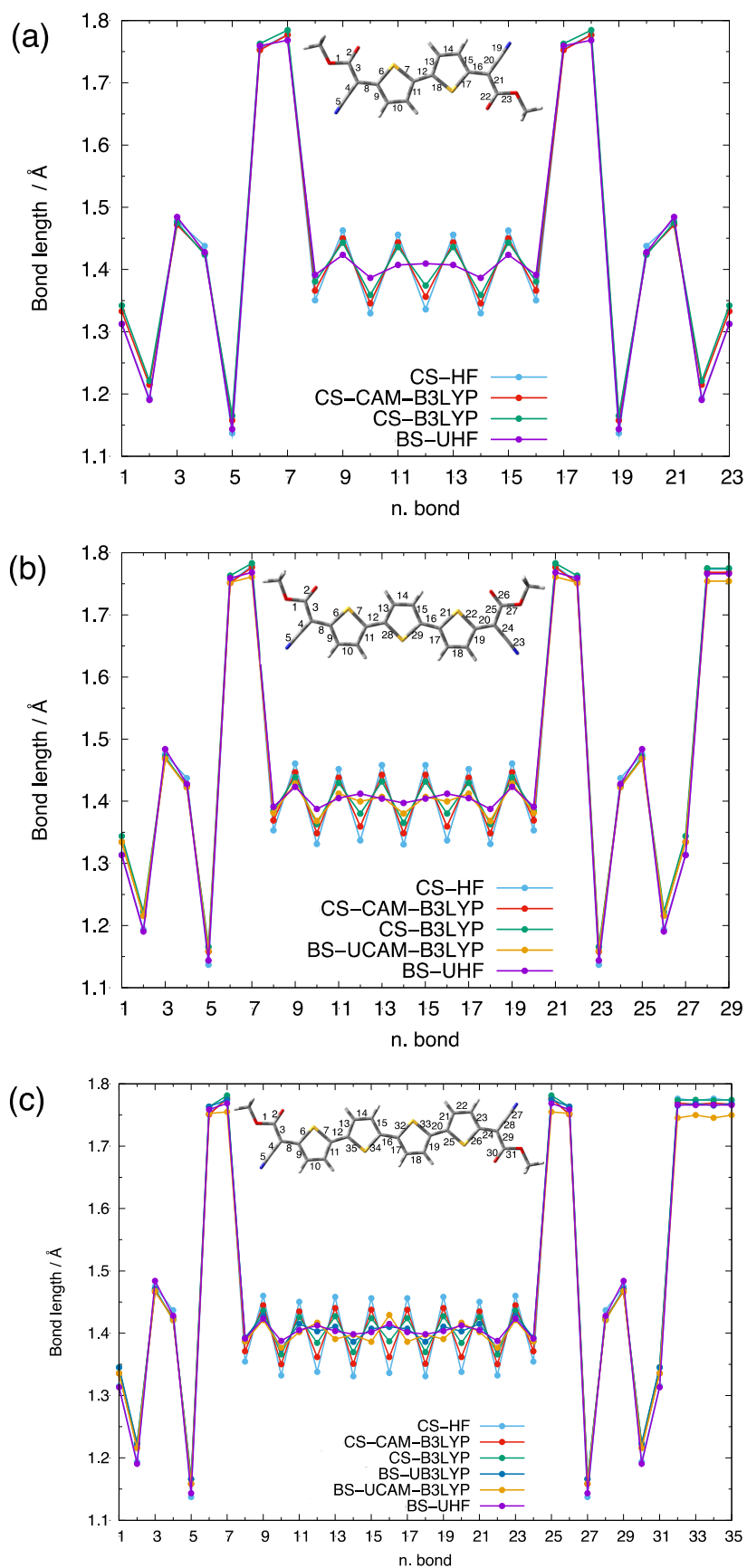


Figure S6. Bond lengths of (a) EsQ2, (b) EsQ3 and (c) EsQ4 calculated at respective optimized geometries. Top center of each panel: bond number definition.

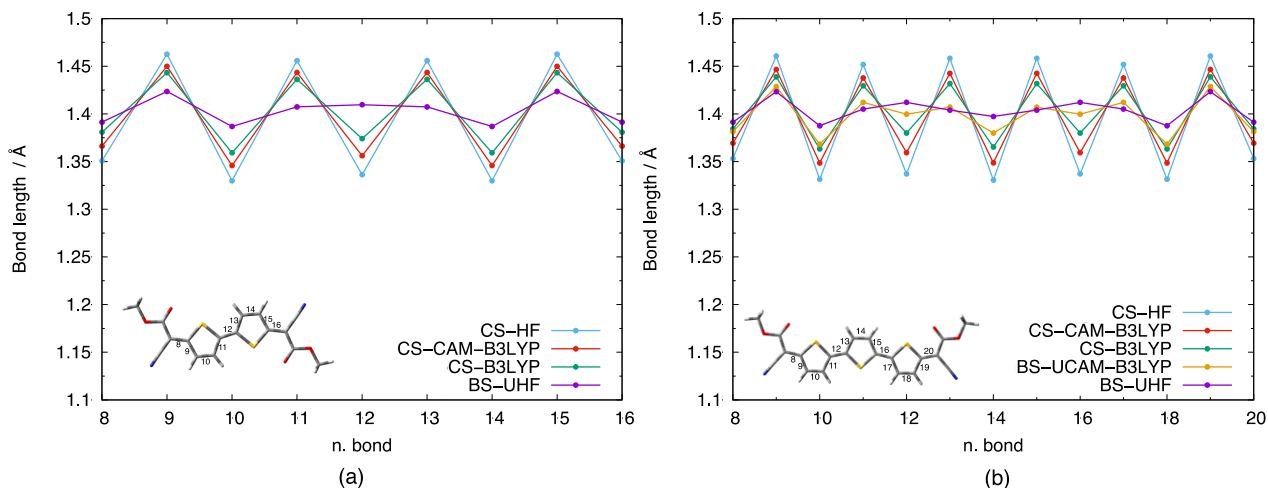


Figure S7. Bond lengths of (a) **EsQ2** and (b) **EsQ3** calculated at CS-HF (cyan), CS-CAM-B3LYP (red), CS-B3LYP (green), BS-UCAM-B3LYP (orange) and BS-UHF (purple) geometries. Bottom left of each panel: bond number definition.

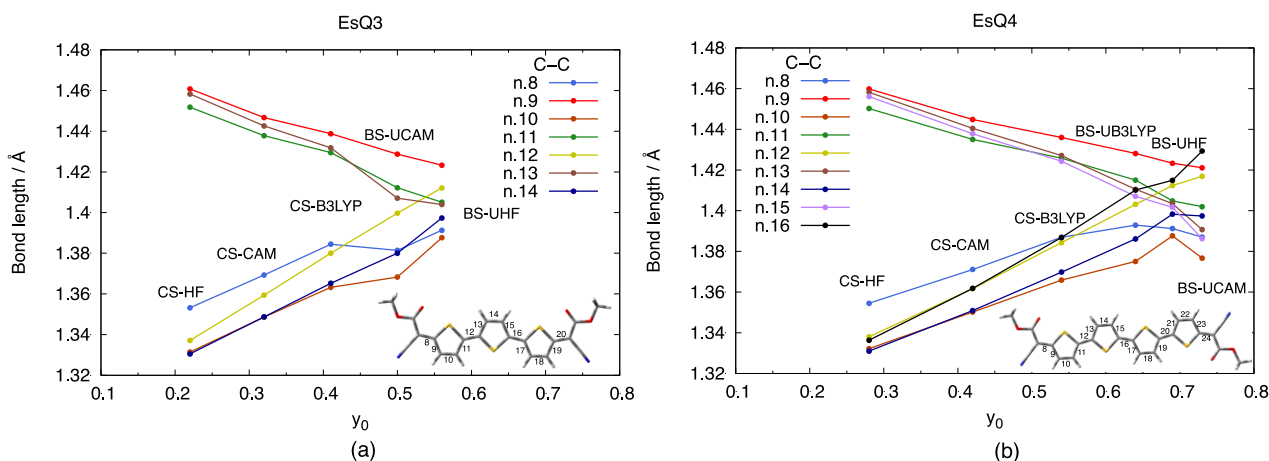


Figure S8. Correlation between C-C bond lengths and y_0^{PUHF} of (a) **EsQ3** and (b) **EsQ4** calculated at different geometries: CS-HF, CS-CAM-B3LYP, CS-B3LYP, BS-UB3LYP, BS-UCAM-B3LYP and BS-UHF. Bottom right: definition of bond number.

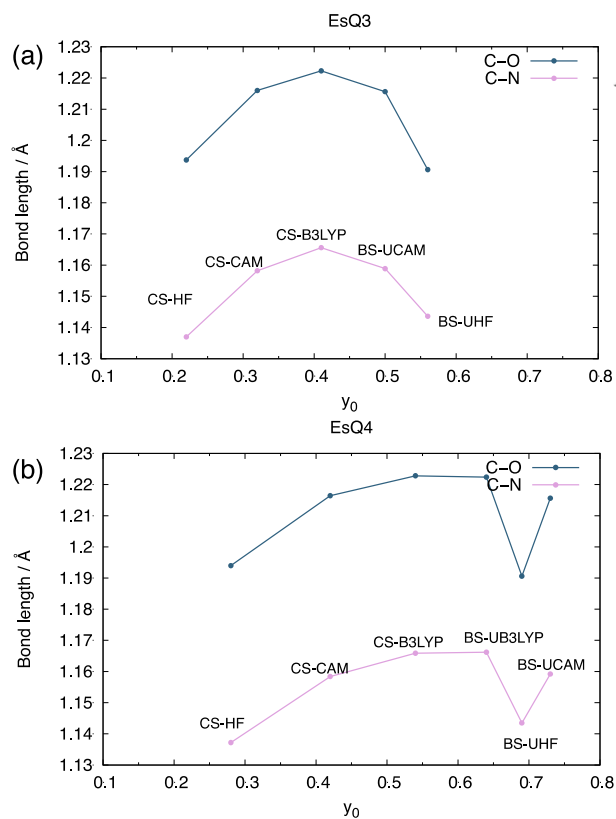


Figure S9. Correlation between C=O and C≡N bond lengths and y_0^{PUHF} of (a) EsQ3 and (b) EsQ4 calculated at available geometries. See Figure 3(a) for the definition of C=O bond.

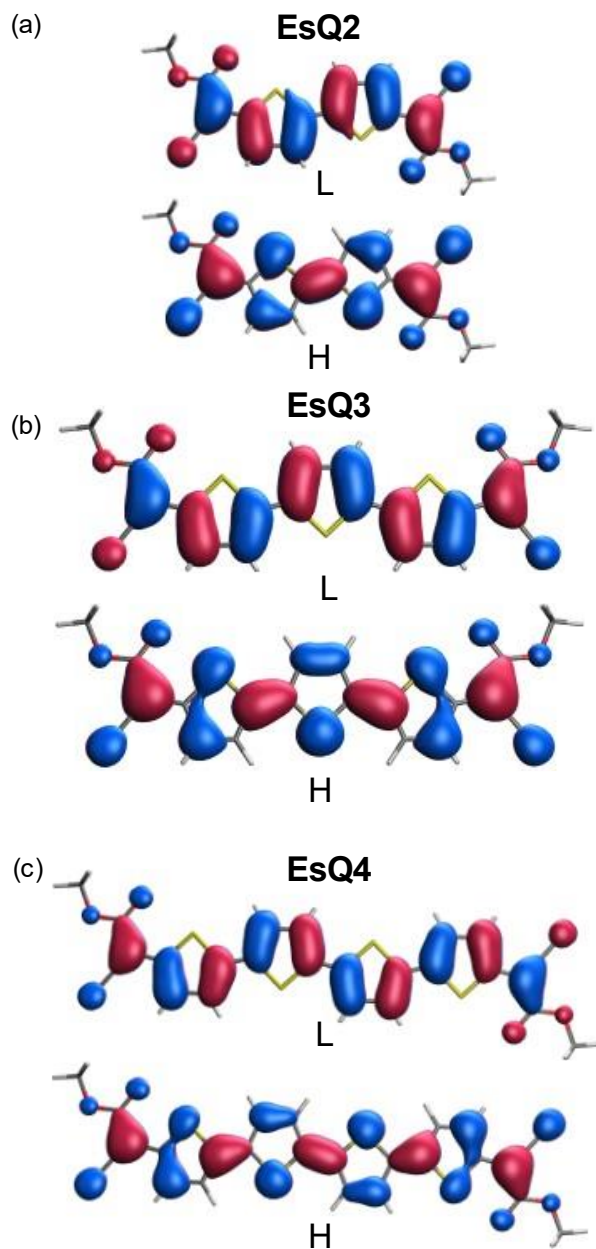


Figure S10. CS frontier orbitals of EsQ2, EsQ3 and EsQ4 from B3LYP/6-31G* calculations.

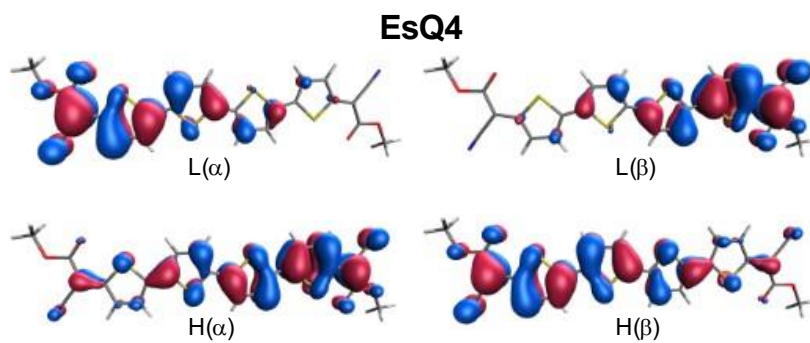


Figure S11. BS frontier orbitals of EsQ4 from UCAM-B3LYP/6-31G* calculations.

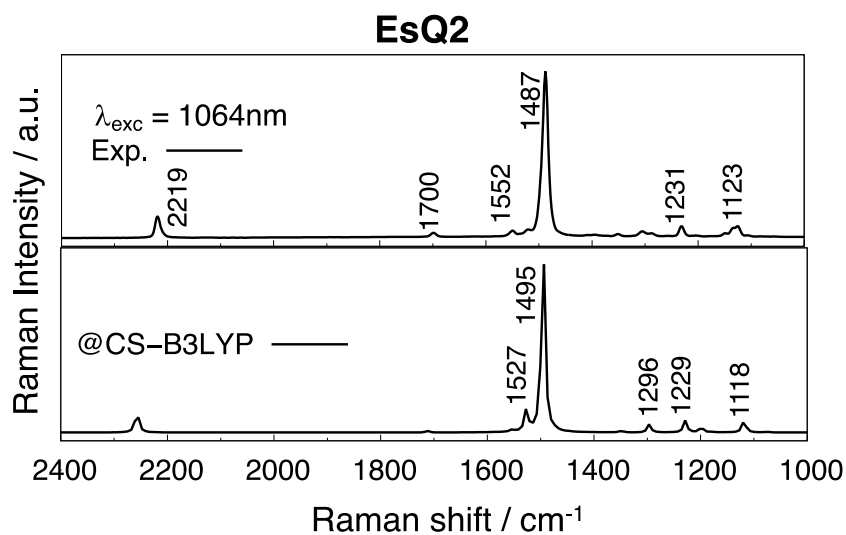


Figure S12. Comparison between experimental and calculated Raman spectra of EsQ2. The experimental spectrum is measured with excitation wavelength of 1064nm. The computed spectrum is obtained at the CS-B3LYP geometry of EsQ2.

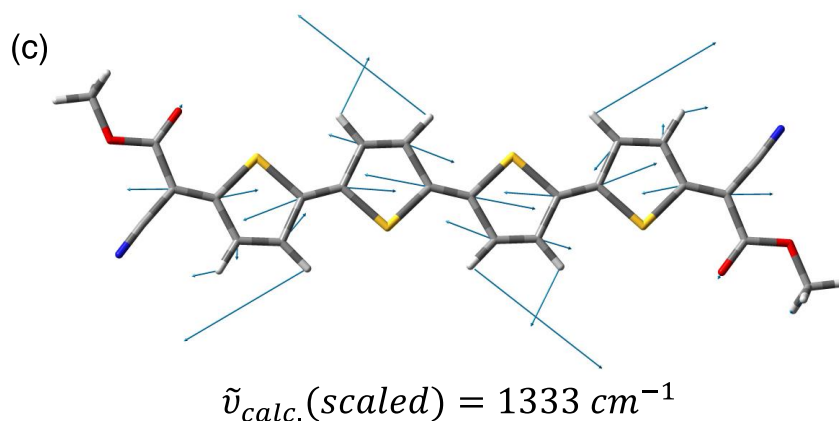
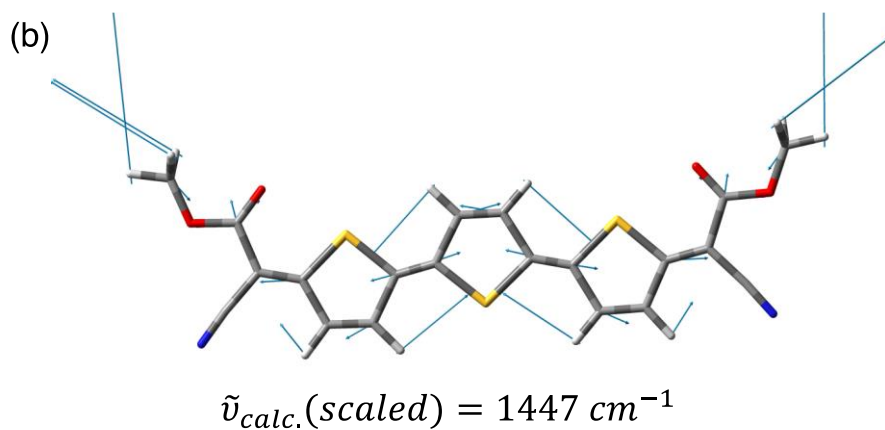
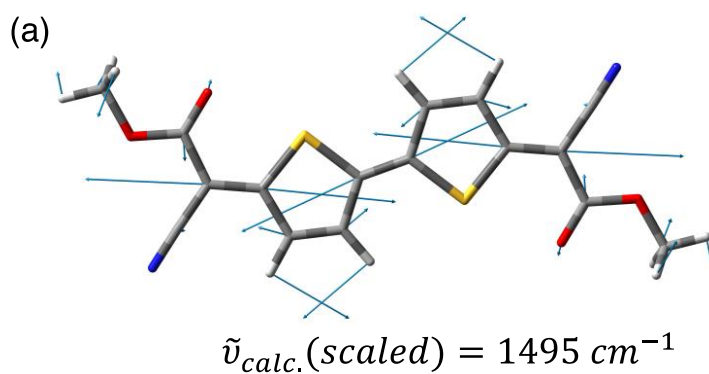


Figure S13. Vibrational modes dominated by the ECC coordinate and associated with the most intense bands of (a) **EsQ2** ($\tilde{\nu}_{Exp} = 1487 \text{ cm}^{-1}$); (b) **EsQ3** ($\tilde{\nu}_{Exp} = 1496 \text{ cm}^{-1}$); (c) **EsQ4** ($\tilde{\nu}_{Exp} = 1356 \text{ cm}^{-1}$); The scaled wavenumbers (scale factor=0.97) calculated at CS-B3LYP geometry (for **EsQ2** and **EsQ3**) and BS-UB3LYP geometry (for **EsQ4**) are reported below each mode representation. Raman spectra calculated at B3LYP/6-31G* level of theory.

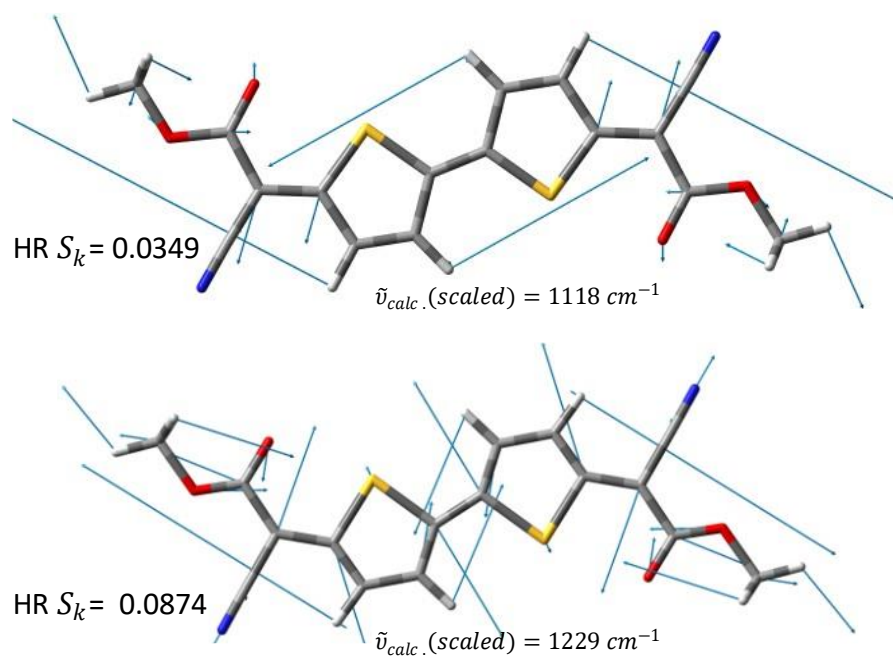


Figure S14. Vibrational modes below 1300 cm^{-1} displaying large HR factors and therefore expected to display enhanced Raman activity in resonance with the optically active transition of **EsQ2**.

EsQ3

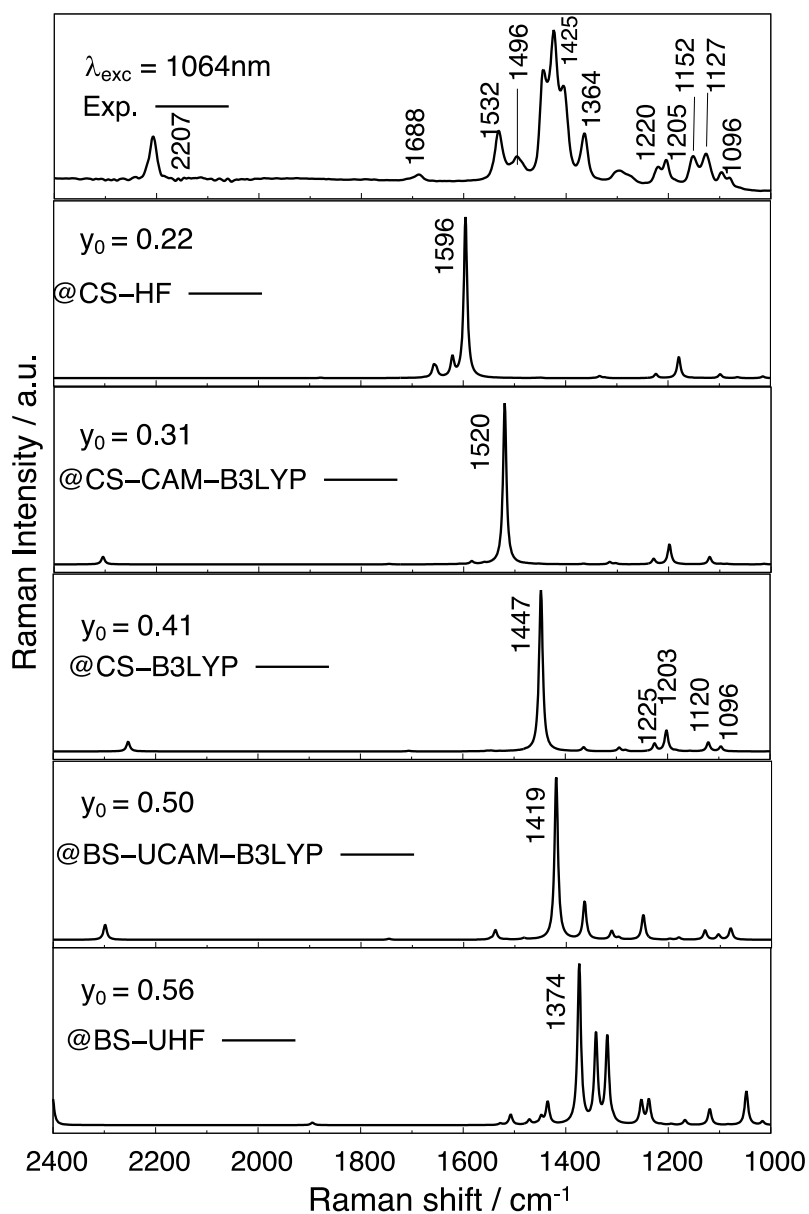


Figure S15. Comparison between experimental (top, spectrum measured at 1064 nm) and computed Raman spectra (B3LYP/6-31G* level of theory) for the library of ground state geometries of **EsQ3** characterized by increasing diradical character as indicated in the top left part of each panel.

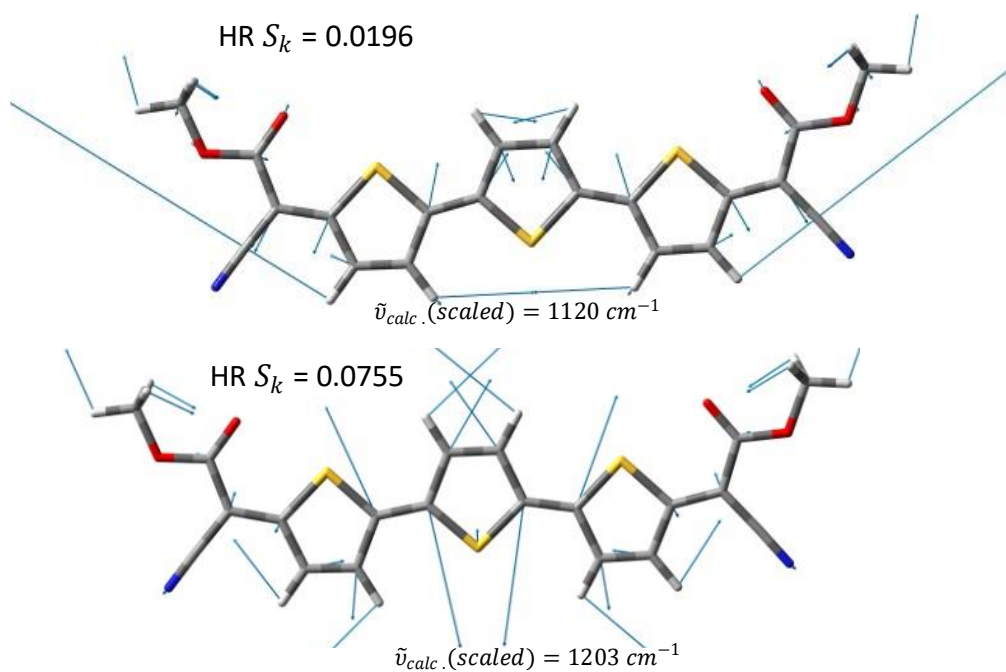


Figure S16. Vibrational modes below 1300 cm^{-1} displaying large HR factors and therefore expected to display enhanced Raman activity in resonance with the optically active transition of **EsQ3**.

EsQ4

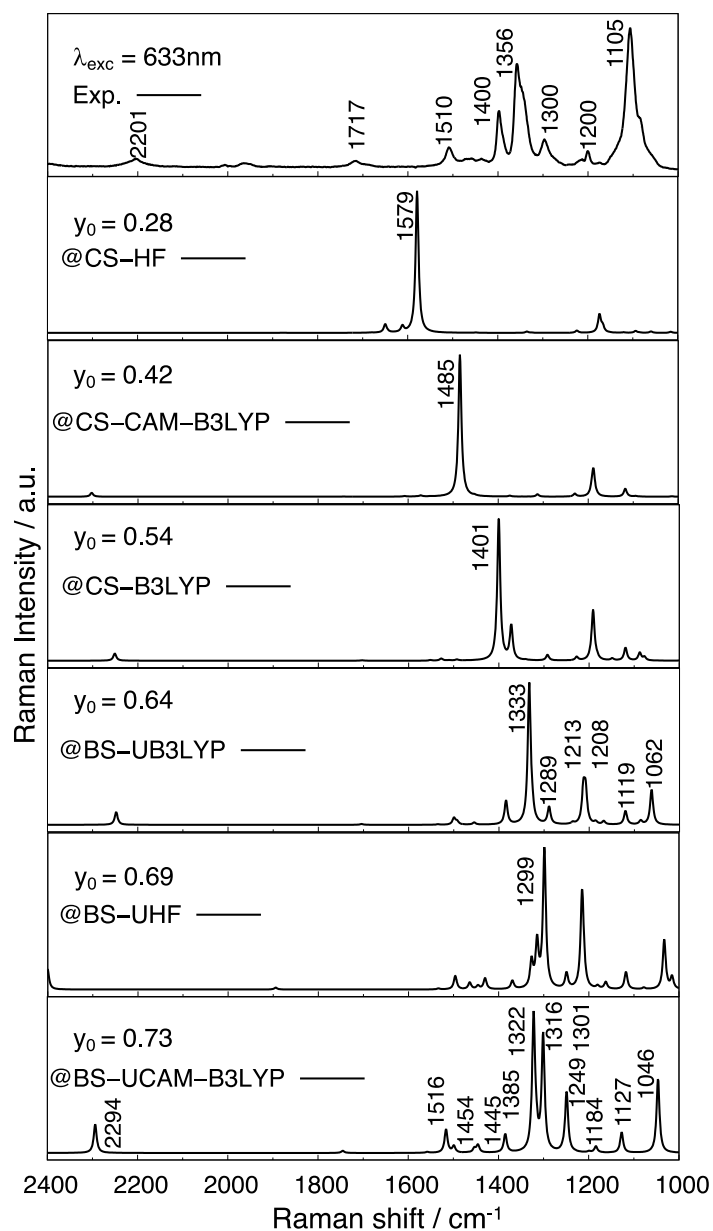


Figure S17. Comparison between experimental (top, spectrum measured at 633 nm) and computed Raman spectra (B3LYP/6-31G* level of theory) for the library of ground state geometries of **EsQ4** characterized by increasing diradical character as indicated in the top left part of each panel.

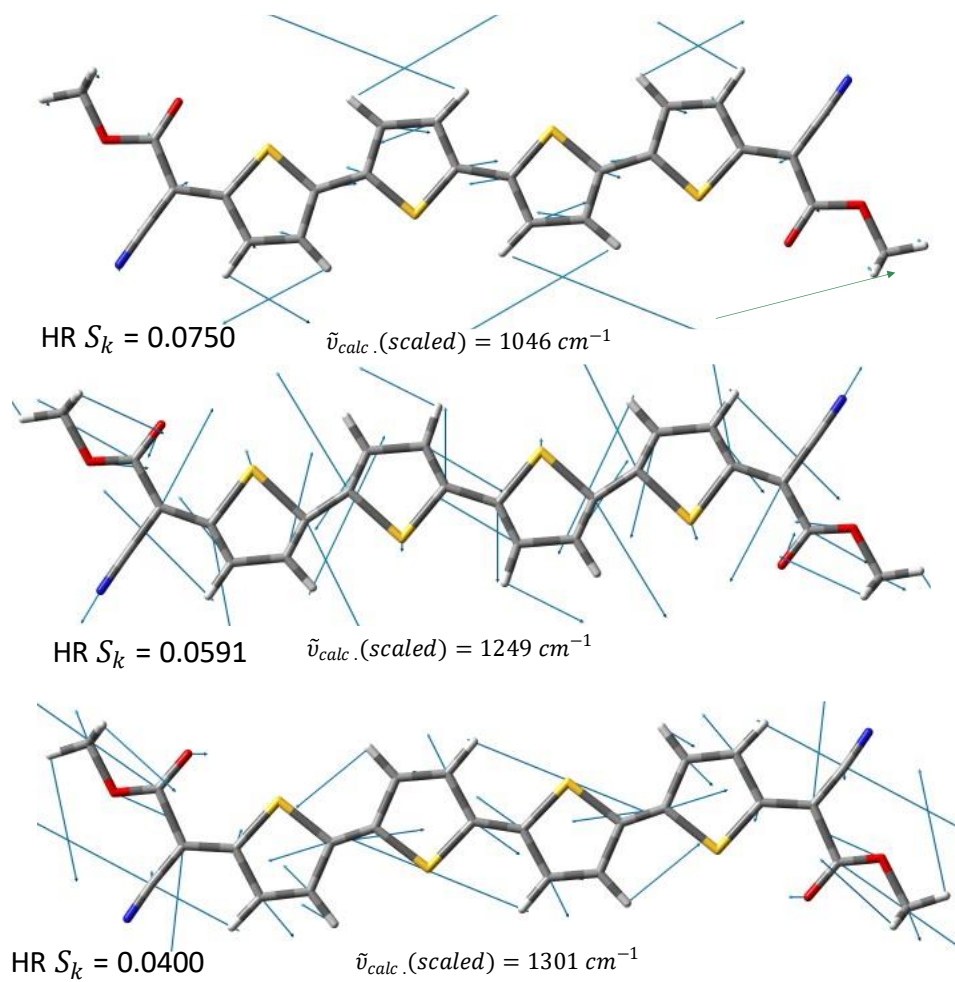


Figure S18. Vibrational modes below 1300 cm^{-1} displaying the larger HR factors and therefore expected to display enhanced Raman activity in resonance with the optically active transition of **EsQ4**.

Table S1. Energy difference (in kcal/mol) between *Conf 1* and *Conf 2* of **EsQ2**, **EsQ3** and **EsQ4** calculated at different geometries.

Energy difference between <i>Conf 1</i> and <i>Conf 2</i> ¹ (kcal/mol)						
Geometry →	CS- HF	CS- CAM-B3LYP	CS- B3LYP	BS- UB3LYP	BS- UCAM-B3LYP	BS- UHF
Molecule ↓						
EsQ2	7.65	7.61	7.57	/	/	7.28
EsQ3	7.90	7.85	7.82	/	8.20	7.45
EsQ4	7.89	7.84	7.79	8.09	8.19	7.38

¹ The energy difference is calculated as $E(\text{Conf } 1) - E(\text{Conf } 2)$

Table S2. N^{FOD} values of **EsQ2**, **EsQ3** and **EsQ4** at available optimized geometries.

N^{FOD}						
Geometry →	CS- HF	CS-CAM-B3LYP	CS-B3LYP	BS-UB3LYP	BS-UCAM-B3LYP	BS- UHF
Molecule ↓						
EsQ2	0.62	0.72	0.80	/	/	0.93
EsQ3	0.89	1.03	1.15	/	1.25	1.31
EsQ4	1.15	1.34	1.49	1.61	1.69	1.66

Table S3. Stabilization energies (kcal/mol) of BS optimized geometries compared to the corresponding CS optimized geometries with the same functional.

Total stabilization energy (CS-BS)		
Molecule	B3LYP/UB3LYP (kcal/mol)	CAM-B3LYP / UCAM-B3LYP (kcal/mol)
EsQ2	/	/
EsQ3	/	2.08
EsQ4	1.00	7.26